Life Sciences 239 (2019) 116999

Contents lists available at ScienceDirect

Life Sciences

journal homepage: www.elsevier.com/locate/lifescie

Transcriptome analysis reveals that cyclophosphamide induces premature ovarian failure by blocking cholesterol biosynthesis pathway

Qi Li[a,1], Xinglan An[a,1], Xiaxia Man[a], Meiran Chu[c], Tianchuang Zhao[c], Hao Yu[b,**], Ziyi Li[a,*]

[a] Key Laboratory of Organ Regeneration and Transplantation of Ministry of Education, First Hospital, Jilin University, Changchun, 130021, China
[b] College of Animal Sciences, Jilin University, Changchun, 130062, China
[c] College of Veterinary Medicine, Jilin University, Changchun, 130062, China

ARTICLE INFO

Keywords:
CTX
POF
RNA-seq
Mice
Transcriptome

ABSTRACT

Aims: The present study aimed to investigate the effects of cyclophosphamide (Cytoxan, CTX) on premature ovarian failure (POF) in mice and its regulatory mechanisms by transcriptome analysis.
Main methods: Female C57BL/6 mice were treated with a single intraperitoneal injection of 70 mg/kg CTX. Serum levels of estradiol (E_2) and follicle stimulating hormone (FSH) were measured by enzyme-linked immunosorbent assay (ELISA), and follicular structure differences were observed by hematoxylin and eosin (H&E) staining. The main mechanism of POF was investigated by RNA-seq data, protein-protein interaction (PPI) networks and qPCR analysis.
Key findings: The serum levels of E_2 were significantly decreased and those of FSH were significantly increased compared to the control group. The ovarian weights of the mice in the CTX group were reduced, and abnormal follicular structures were also observed in the CTX group. The RNA-seq data show that the downregulated genes were related to the cholesterol biosynthesis pathway. The PPI network and qPCR analyses further confirm that the PPAR signaling pathway and the ovarian infertility genes were also involved in blocking the cholesterol biosynthesis pathway. The differences were statistically significant.
Significance: Our results indicate that CTX may exert its anti-tumor effects by inactivating the cholesterol biosynthesis pathway, and simultaneously reducing the supply of estrogen precursor materials, ultimately leading to the occurrence of POF. Our data provided a preliminary theoretical basis for resolving the clinical toxicity and side effects of CTX.

1. Introduction

Although the treatment methods for cancer are more and more diversified, chemotherapy is still the most common treatment method for cancer patients, followed by surgery, radiotherapy and other more professional treatments [1]. Since the first attempt to treat Hodgkin's disease with alkylating agent, cancer chemotherapy has made great progress. As the most widely used alkylating agent and anti-tumor drug, cyclophosphamide (CTX) is always in dispute because of its side effects [2]. CTX is clinically used to treat malignant lymphoma, multiple myeloma, breast cancer, lung cancer, childhood tumors, and many solid tumors [3]. In addition, CTX has also achieved satisfactory clinical results in the treatment of immunosuppression, steroid dependence and localized segmental glomerulosclerosis (FSGS) [4]. CTX used to treat cancer are undoubtedly beneficial. However, CTX can cause strong alkylation of chloroethyl phosphoramide under the catalysis of liver microsomale enzymes, which produce cytotoxic effects on tumor cells. Among various toxicity and side effects of CTX, its damage to ovaries has attracted much concern, this damage is frequently associated with premature ovarian failure (POF) and infertility due to ovarian germ cell toxicity. Its side effects on the quality of life of female cancer survivors and their offspring cannot be ignored [5].

CTX has the greatest POF risk among all chemotherapeutic drugs [6–8]. POF is a heterogeneous disorder that occurs in women before the age of 40, and is characterized by primary and secondary amenorrhea, low estrogen levels and high gonadotropin levels [9]. It is also a common cause of infertility in women. Animal studies have shown that chemotherapy can cause the significant loss of dormant primordial

* Corresponding author.
** Corresponding author.
E-mail addresses: liqi910224@163.com (Q. Li), anxinglan@jlu.edu.cn (X. An), 110034068@qq.com (X. Man), 12688347@qq.com (M. Chu), zhaotianchuang@2008.sina.com (T. Zhao), yu_hao@jlu.edu.cn (H. Yu), ziyi@jlu.edu.cn (Z. Li).
[1] These authors contributed equally to this work.

https://doi.org/10.1016/j.lfs.2019.116999
Received 10 August 2019; Received in revised form 16 October 2019; Accepted 18 October 2019
Available online 23 October 2019
0024-3205/

follicles and growing follicles. The CTX toxicity to the ovaries is mainly the damage to the primitive follicles and sinus follicles, and this destroys them in a time - and dose-dependent manner. The loss of primordial follicles is the main determinant of ovarian failure, because these follicles are the source of all follicles in the ovarian life cycle, and the pool of these follicles is finite. There is a controversy as to the target cells of CTX in ovarian follicles. Some supporters believe that chemotherapy drugs seem to directly target oocytes in primordial follicles and primary follicles for apoptosis and destruction [10,11]. Women who receive CTX always have a high risk of permanent amenorrhea and premature menopause. Ovarian pathology usually shows a primordial follicle pool in these patients, with reduced ovarian vascular damage and ovarian atrophy [12]. Recently, CTX is now being used in combination with various detoxifying and protective agents with the purpose of reducing or eliminating its ovarian toxicity [13]. It is well known that rapidly dividing cells are more sensitive to cytotoxic effects of alkylating agents than stationary cells. This makes follicular steroid-producing cells a possible target for CTX [14]. However, the underlying pathogenesis mechanisms of CTX-induced POF development are complex and remains to be elucidated, and there is no effective treatment.

Therefore, the aim of this study was to explore potential molecular pathogenesis of CTX-induced POF on the mice models by RNA-seq technology, and the results of this essential experiment will provide a theoretical basis for finding suitable antidotes.

2. Materials and methods

2.1. Experimental animals

Female C57BL/6 mice at 6–8 weeks of age, were obtained from Liaoning Changsheng Biotechnology Co. Ltd. To explore the effects of the drugs on ovarian injury in mice, the experiment was divided into 2 groups, 8 mice in each group. The mice were administered a single intraperitoneal injection of 70 mg/kg CTX (Sigma, USA), the control group received equivalent doses of normal saline solution. At 14 days, the mice were sacrificed by cervical dislocation. The current study received ethical approval from the Animal Ethics Committee of Jilin University (Approval ID:20151008–1) in compliance with the Experimental Animal Regulations of the National Science and Technology Commission in China.

2.2. Enzyme-linked immunosorbent assay (ELISA)

At 14 days, mouse blood plasma was obtained by mouse retro-orbital blood collection. Blood samples were incubated at 37 °C for 1 h, centrifuged at 3000 rpm at 4 °C for 10 min, and the supernatant was collected. The serum levels of estradiol (E_2) and follicle-stimulating hormone (FSH) were measured by ELISA kits (Westang Bio, China) according to the manufacturer's instructions. For E_2, functional sensitivity was 18 pg/ml and intra-assay and inter-assay coefficients of variation (CV) were 4% and 4% respectively. For FSH, functional sensitivity was 1 ng/ml and intra-assay and inter-assay CV were 10% and 10% respectively. Then, 100 μl standards were prepared at the following concentrations: E_2, 1400, 700, 350, 120, 40, 20, 10 and 0 pg/ml; FSH, 25, 12.5, 6.25, 3.12, 1.56, 0.78, 0.39, 0.195 and 0 ng/ml, the prepared standards and diluted mouse plasma were added to microtest wells that were precoated with anti-E_2 or anti-FSH antibodies, and the samples were incubated for 40 min. The plates were washed 4–6 times with wash buffer, added the biotinylated antibodies, and incubated for 20 min. Then added the enzyme conjugates, incubated for 10 min, TMB solutions were added and the plates were incubated for 15 min in the dark. This was followed by the addition of a stop solution. The optical absorbances were determined at a wavelength of 450 nm using a microplate reader (Bio-Tek, USA).

2.3. Hematoxylin and eosin (H&E) staining and ovarian follicle counting

The ovarian tissues were collected and washed 3 times with phosphate-buffered saline (PBS), fixed with 4% paraformaldehyde (Sigma, USA) for 30 min, dehydrated using a graded series of ethanol, vitrified in xylene and embedded in paraffin (both purchased from Sigma, USA). Next, serial 6 μm thick sections (Leica, Germany) were made and stained with hematoxylin and eosin (Sigma, USA). All samples were observed under a Nikon Eclipse Ti–U microscope (Nikon, Japan). Color images were captured using a DS-Ri2 CCD camera (Nikon, Japan).

Three ovaries were collected in CTX group and control group, respectively. The seventh slice from each ovary were chosen to calculate the number of follicles. The follicles were categorized as primordial, primary, secondary and atretic follicles, according to the method described previously, oocytes whose follicles are surrounded by a layer of partially or intact squamous granules are classified as primordial follicles. The primary follicle shows a single layer of cubic granulosa cells. If the follicle has more than one layer of granulosa cells without visible antrum, it is classified as a secondary follicle. The follicular wall collapses, and the separation of granulosa cells from oocytes is classified as atretic follicle [15].

2.4. RNA isolation and sequencing

The total RNA from the ovarian tissues was extracted with TRIzol Reagent (Life Technologies, USA) using RQ1 RNase-free DNase (Promega, USA) to remove the genomic DNA. RNA-sequencing was performed by GENEWIZ using an Illumina HiSeq sequencer (Illumina HiSeq 2000 platform). Raw and processed RNA-seq data were deposited at GEO DataSets: GSE128240.

2.5. Integrated analysis of microarray datasets

The Limma package [16] was applied to perform the normalization and log2 conversion of the dataset. $|\log2FC| > 1$ and an adjusting FDR cutoff of 0.05 were considered statistically significant for the DEGs.

2.6. Functional enrichment analysis

The pathway enrichment for the upregulated and downregulated differentially expressed genes (DEGs) was performed via WEB-based Gene Set Analysis Toolkit[https://webgestalt.org/]. Select genes that were associated with the cholesterol biosynthesis pathway were enriched using Network Analyst [http://networkanalyst.ca]. The pathways were generated from the pathway enrichment results, and the transcriptome expression data generated by pathvisio were integrated.

2.7. Protein-protein interaction (PPI) network construction

To demonstrate the potential PPI relationship, the DEGs were mapped to the PPI data that were collected from the cholesterol biosynthesis, PPAR signaling pathway and ovarian infertility genes subdata sets of the pathway enrichment. The Pearson correlation coefficient (PCC) [17] was calculated for all pair-wise comparisons of gene expression values between the normal genes and the DEGs. The PPI relationships absolute PCCs are larger than 0.4 were considered as significant. Then, the PPI networks were constructed using Cytoscape [18] based on the PPI relationships [19].

2.8. Reverse transcription and quantitative PCR (qPCR)

The RNA was reverse transcribed into cDNA using TransScript All-in-One First-Strand cDNA Synthesis SuperMix (Transgen, China) according to the manufacturer's instructions. In brief, first-strand cDNA was synthesized in 20 μl reactions from 2 μl total RNA using SuperMix and RT reaction steps consisted of 42 °C for 15 min and 85 °C for 5 s.

Table 1
Primers for the mRNAs.

Gene	Accession no.	Primer sequence	Annealing temp.(°C)	Product size(bp)
Adipoq	NM_009605	F: 5′-GAGTCCTGAGTATTATCCA-3′ R: 5′-CATTCTGTTATTGCTACCA-3′	56	135
APOA1	NM 009692	F: 5′-CATTTCTGGCAGCAAGATGA-3′ R: 5′-TCACCTCCTCCAGATCCTTG-3′	61	75
PCK1	NM 011044	F: 5′-CTGGATGAAGTTTGATGCCC-3′ R: 5′-TGTCTTCACTGAGGTGCCAG-3′	61	159
CYP19A1	NM_001348171	F: 5′-CAATAAGATGTATGGAGAGTTC-3′ R: 5′-CTTGAGGACTTGCTGATAA-3′	58	75
GDF9	NM_008110	F: 5′-ACAGATGGATTGAGATTGA -3′ R: 5′-ATTGACAGACAGGTGAAT-3′	57	78
FSHR	NM_013523	F: 5′-TATTAGACATTCAAGATAACATAA-3′ R: 5′-ATCGCTTAGATTCAGTTC-3′	55	164
SQLE	AK138457	F: 5′-TTCCACTCATCTATTCAG-3′ R: 5′-GACACAGTTCTATGCTAT-3′	54	108
CYP51A1	NM 000786	F: 5′-TGGAGCGAAAAGTCCACCAC-3′ R: 5′-TGCATCACTCCCCAGAAGGTA-3′	61	76
HMGCR	NM 008255	F: 5′-GCTTGTGAGAAGGAACCA-3′ R: 5′-GCTCTGCTTGTAGTCTCTG-3′	61	104
HMGCS1	AK044835.1	F: 5′-GTTGGAGGAATGGATGTC-3′ R: 5′-AGTTCAGTTCAGCAGAGA-3′	59	121
DHCR7	AK190502	F: 5′-GCCATTGAGTGCTCCTACA-3′ R: 5′-ACCCCAGAAGCCTGAGAC-3′	64	75
FDPS	AK140881	F: 5′-AGTTCCTATCAGACAGAG-3′ R: 5′-TTCAGTGTATCTACCAAGA-3′	56	84
β-actin	NM 001101	F: 5′-CCTCTATGCCAACACAGT-3′ R: 5′-TAGGAGCCAGAGCAGTAA-3′	60	250

Real-time PCRs were conducted with FastStart Essential DNA Green Master (Roche, USA) and the LightCycler® 96 Instrument (Roche, USA) according to the manufacturer's instructions. The 20 μl reaction mixtures consisted of 8 μl water, 1 μl cDNA, 1 μl (10 μM) primers and 10 μl FastStart Essential DNA Green Master. The thermocycling program consisted of 95 °C for 180 s, followed by 40 cycles at 95 °C for 10 s, 60 °C for 30 s, then 95 °C for 30 s, 65 °C for 60 s and 97 °C for 1 s, and a final step at 37 °C for 30 s. The relative expression of each gene was analysed using the $2^{-\Delta\Delta Ct}$ method. β-actin was used as the reference gene. The primer sequences used in the experiments are listed in Table 1.

2.9. Statistical analysis

Each experiment was biologically replicated at least three times. The data were analysed with Prism (GraphPad, LA Jolla, CA) by *t*-test. A value of $p < 0.05$ was considered significantly different, and $p < 0.01$, $p < 0.001$ was considered extremely significantly different. (*$p < 0.05$, **$p < 0.01$, ***$p < 0.001$).

3. Results

3.1. Detection of E_2 and FSHby ELISA

ELISA was used to detect the serum levels of E_2 and FSH in the blood of mice in CTX group and control group, as shown in Fig. 1. Compared with the control group, we found that the serum level of E_2 in the CTX group decreased by approximately 40%, while the serum level of FSH increased by approximately 3 times, indicating that the dose of CTX used in this experiment had a significant effect on the estrogen levels in the mice.

3.2. H&E staining of ovarian tissue and ovarian follicle counting

The ovaries of the mice in the CTX group and the control group were collected for pathological analysis. The sizes of the ovaries and fallopian tubes were found to be reduced in the CTX group compared with those of the control group by observing their external morphology (Fig. 2A–B). The weights of the ovaries in the CTX group were decreased by approximately 44% when compared with that of the control group (Fig. 2C). We further observed the histological structure of the ovaries by H&E staining , the results show that there was a significant difference between that of the CTX group and the control group (Fig. 2D

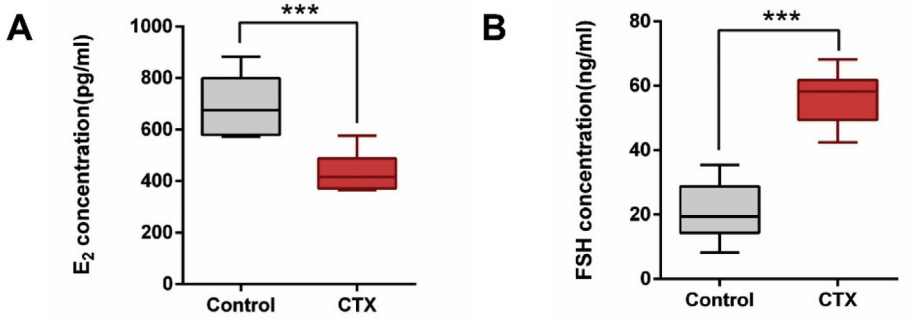

Fig. 1. Serum levels of E_2 and FSH in the CTX group. (A) Plasma E_2 levels were determined by ELISA. (B) Plasma FSH levels were determined by ELISA. Data are presented as the mean ± SD. ***$P < 0.001$ vs control group.

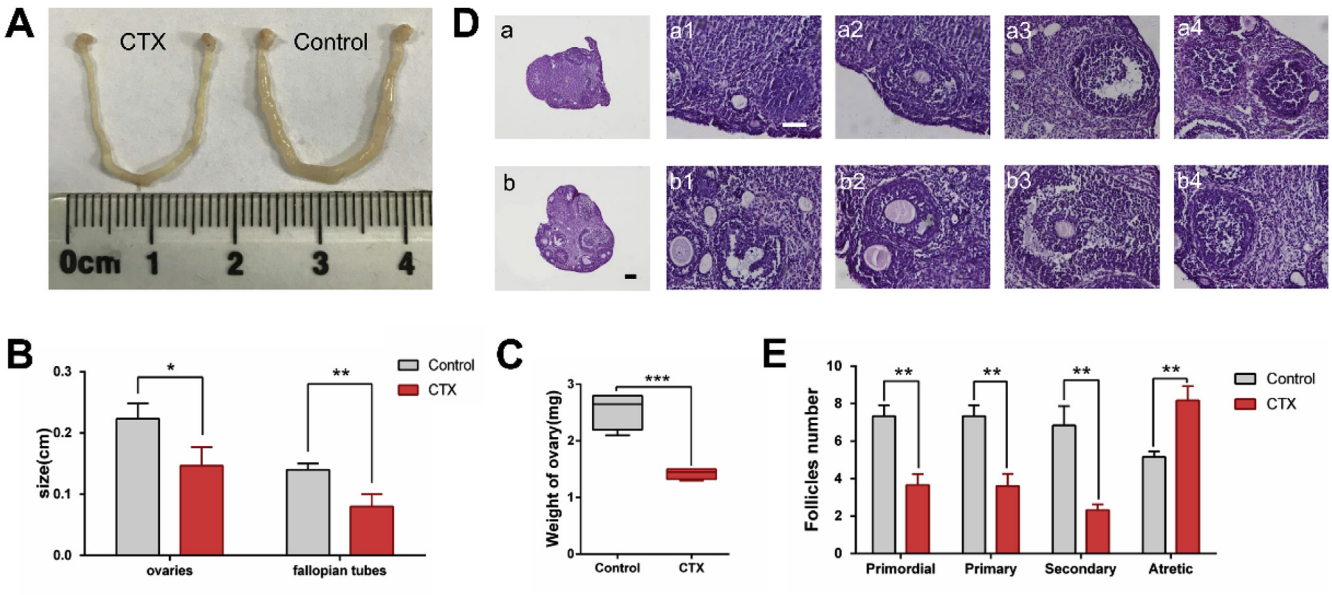

Fig. 2. Pathological analysis of the CTX group and the control group. (A) Female mouse reproductive organs (ovaries, fallopian tubes and uterus). (B) The size of the ovaries and fallopian tubes in the CTX group and the control group. (C) The weights of the ovaries in the CTX group and the control group. (D) The pathological observation of ovaries from the CTX group and the control group. (a–b) CTX group (a) and the control group (b), Scale bar = 500 μm, (c–j) follicles at the four following periods in the CTX group and the control group: primordial follicle (a1, b1), primary follicle (a2, b2), secondary follicle (a3, b3) and atretic follicle (a4, b4), Scale bar = 200 μm. (E) The quantitation of the follicle counts from the ovaries in the CTX group and the control group. Data are presented as the mean ± SD. *p < 0.05, **P < 0.01, ***P < 0.001 vs control group.

(a-b)). There were differences in follicular structure and number between the CTX group (Fig. 2D (a1-a4) and the control group (Fig. 2D (b1-b4)) at the four following periods: primordial follicle, primary follicle, secondary follicle and atresia follicle. In contrast, the ovaries of the CTX group are mainly composed of mesenchymal cells in the fibrous matrix (Fig. 2C–a). Compared with the control group, the number of functional follicles (primordial follicles, primary follicles and secondary follicles) in the CTX group was significantly reduced by approximately 50%, 51% and 66% respectively, while the number of atresia follicles increased significantly by approximately 58%, as shown in Fig. 2E.

3.3. Identification of differentially expressed genes (DEGs) in the CTX group

A total of 874 DEGs were obtained for the CTX group compared with the control group, which included 490 upregulated DEGs and 384 downregulated DEGs, as shown in the volcano plot (Fig. 3A) and heatmap (Fig. 3B).

3.4. Pathway enrichment analysis

KEGG pathway enrichment based on gene set enrichment analysis (GSEA) methods for DEGs was performed by using WebGestalt, and we observed that only the downregulated genes were significantly enriched in the cholesterol biosynthesis pathway (NES > 1, log10 of FDR > 2). A volcano plot of pathway enrichment showed that the differences in enrichment between the cholesterol biosynthesis pathway and the others were very obvious, the PPAR signaling pathway and the ovarian infertility genes were also enriched in the top 10 pathways of

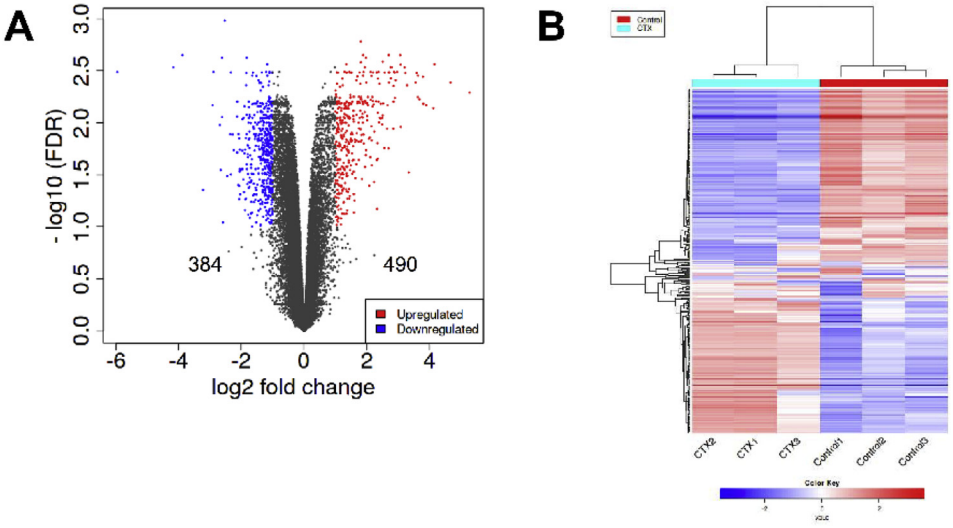

Fig. 3. Differentially expressed genes (DEGs) in the CTX group. (A) A volcano plot of the gene expression profile data in the CTX group and the control group. (B) The expression of DEGs displayed by a heatmap in the CTX group and the control group.

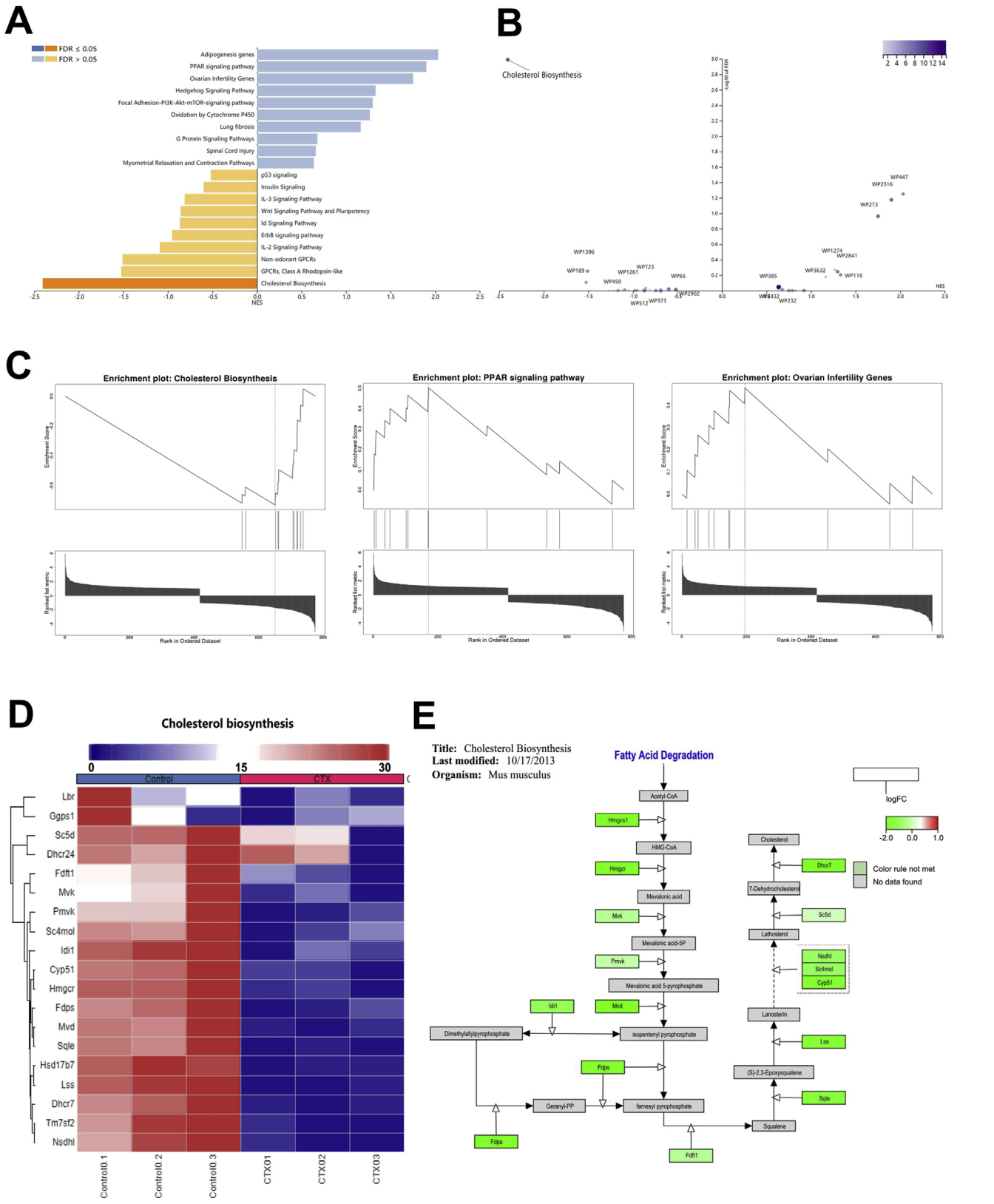

Fig. 4. Functional enrichment analysis of DEGs. (A) The pathway enrichment analysis for the upregulated and downregulated DEGs. (B) A volcano plot of the pathway enrichments in the CTX group and the control group. (C) GSEA analysis of the cholesterol biosynthesis pathway, the PPAR signaling pathway and the ovarian infertility genes. (D) The expression of the DEGs of the cholesterol biosynthesis pathway displayed by a heatmap of the CTX group and the control group. (E) The enrichment of the gene expression level of the cholesterol biosynthesis pathway in the CTX group.

upregulated gene enrichment, which are two reported cholesterol-related pathways, as shown in Fig. 4A and B. In the GSEA pathway enrichment plots of the three pathways, we found that there was almost no significant upregulation of any of the background genes in the cholesterol biosynthesis pathway (Fig. 4C). This result was further demonstrated through a GSEA heat map and pathway diagram, which indicate that the inhibition of cholesterol biosynthesis is one of the significant consequences of CTX (Fig. 4D and E).

3.5. PPI network construction and validation of hub genes by qPCR

We selected the upregulated genes of two pathways, including the PPAR signaling pathway and the ovarian infertility genes, the downregulated genes of the cholesterol biosynthesis pathway to construct a PPI network. We found that the PPI network was formed by integrating the main network of the SQLE-dominated cholesterol biosynthesis pathway as the core with two relatively independent sub-networks: the PPAR signaling pathway and ovarian infertility genes. Among the downregulated genes, the node connectivity of 11 downregulated genes was very high ($n \geq 10$). In the upregulated genes, the top 3 hub genes in the PPAR signaling pathway were *Adipoq*, *APOA1* and *PCK1* ($n \geq 7$), in the ovarian infertility genes pathway. The top 3 hub genes are *CYP17A1*, *GDF9* and *FSHR* ($n \geq 6$) (Fig. 5A).

To verify the RNA-seq results, the hub genes were selected for qPCR detection. These genes were found to have a significantly differential expression pattern between the CTX group and the control group, except for *PCK1*, as shown in Fig. 5B and C. The qPCR results were similar to those of the RNA-seq analysis, as expected. While the differential expression level of the *Adipoq* gene is much higher than that of the other genes, its expression level increased by approximately 78 times.

4. Discussion

CTX is the first so-called “latent” broad-spectrum anti-tumor drug, which has effects on leukaemia and solid tumors. It is inactive in vitro and mainly hydrolysed to aldehyde phosphoramide by liver microsomal cytochrome P450 in the body [20,21], specifically, the enzymes in the tumor cells due to a lack of normal tissue cells. It can be decomposed into phosphoramide mustard that is highly toxic to tumor cells, thereby playing an anti-tumor effect. However, it also has toxic effects will damage ovaries and has obvious teratogenic and mutagenic effects, especially for cell division and development of organs in embryos. The embryos are absorbed, stunted, or deformed, and these deformations may include abnormal limbs or a cleft palate [22,23].

It has been reported that different doses of a single injection of CTX have different effects on ovarian [24]. In a previous report, superovulation after injected a single dose of 50 mg/kg CTX for 100 h in mice [25]. In another report, follicular growth initiated by CTX at a single dose of 200 mg/kg began to decline [26]. Recent studies have shown that a single dose of 70 mg/kg CTX causes POF [27–30] found that the serum levels of FSH in the CTX group were increased, but the E_2 level was reduced. The weights of the ovaries in the CTX group were also obviously reduced. Compared with the control group, the morphology of the ovaries in the CTX group was changed, and the number of functional follicles was decreased significantly, but the number of atresia follicles was increased. In our study, we injected a single dose of 70 mg/kg CTX in mice to analyse the effects of CTX on POF mouse model as well as its potential mechanism to cause ovarian injury. Our experiments confirmed that 70 mg/kg CTX was effective in inducing POF in mice. Based on this, we continued to investigate the pathogenesis of POF induced by CTX with RNA-seq technology.

Thus far, FSH and E_2 are considered to be the most relevant risk factors for the occurrence of POF. FSH induces ovarian follicles maturation by acting on the FSH receptors (FSHRs) expressed on granulosa cells [31,32]. The development of follicles and the differentiation of mesenchymal cells around mature follicles into two layers of follicular membrane cells because of the action of FSH. Follicular membrane cells secrete androgens, which are converted into estrogens by the activation of an aromatase, such as *CYP19A1* in granulosa cells [33,34]. The increase in FSH levels is mainly due to the low levels of ovarian steroids and peptides, and the inability to inhibit pituitary FSH secretion by negative feedback [35]. Previously, POF was detected in patients clinically younger than 40 years old, and the researchers found that the patients’E_2 levels were lowered and the serum FSH levels were elevated

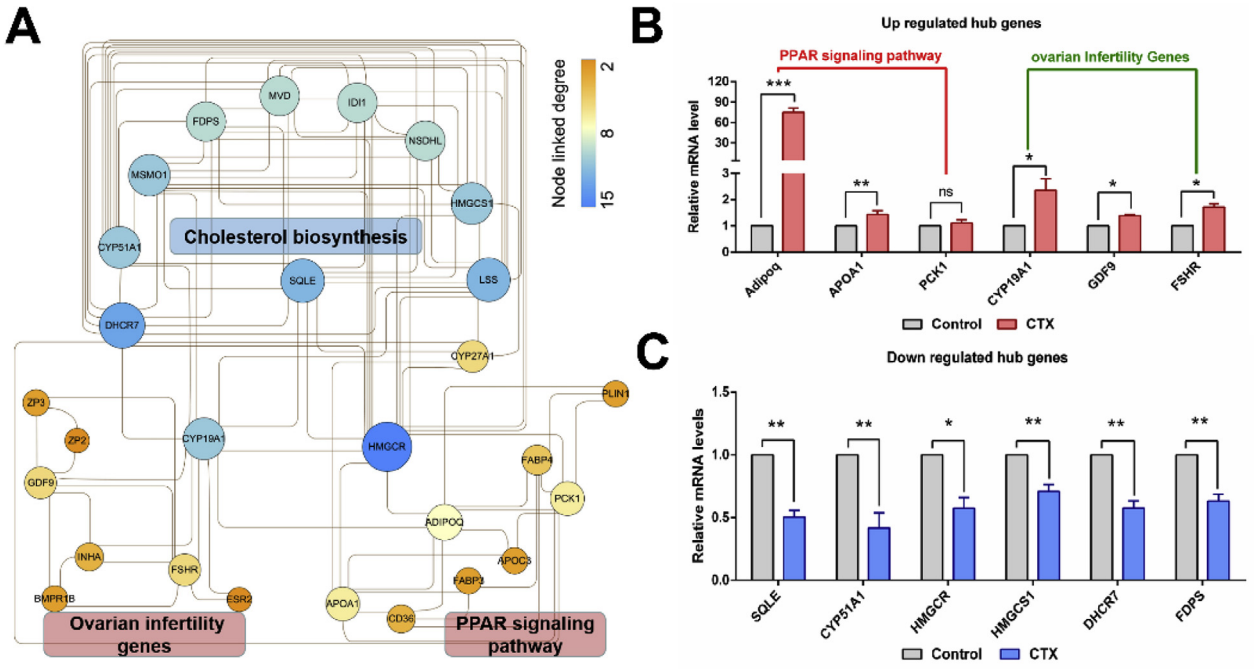

Fig. 5. PPI network construction and expression of selected genes in the CTX and control groups. (A) Upregulated gene-downregulated gene networks in the CTX group. (B) The expression levels of 6 upregulated genes in the CTX and control groups by qPCR. (C) The expression levels of 6 downregulated genes in the CTX and control groups by qPCR. Data are presented as the mean ± SD. *p < 0.05, **P < 0.01, ***P < 0.001 vs control group.

[9,36]. Wang et al. reported that 6-week-old ICR mice were injected with CTX to construct a POF mouse model, and E_2 was found to be significantly reduced [37]. In our study, we found that the serum concentration of FSH was indeed elevated, and the qPCR results also show that the expression of FSHR was increased. However, the E_2 is required for ovarian development and maturation was reduced. E_2 is mainly secreted by the ovaries, follicles, corpus luteum and placenta during pregnancy [38]. It is the most important and biologically active type of estrogen, and a lack of E_2 is considered to be the most important pathogenic factor of POF.

It is well known that sex hormones are mainly synthesized by cholesterol, and the most primitive precursor of E_2 synthesis is also the conversion of cholesterol into pregnenolone, so the reduction of cholesterol biosynthesis will directly hinder the reduction of E_2 production and will directly lead to POF under the promotion of FSH.

Located in the endoplasmic reticulum, *SQLE* is one of the key rate-limiting enzymes in the first step of cholesterol biosynthesis oxidation [39]. Previous studies have found that *SQLE* is closely related to the occurrence and development of breast cancer, lung cancer, colorectal cancer and other tumors [40–43]. Sui et al. reported an increase in the expression of *SQLE* in hepatocellular carcinoma cells, that promote cell growth and migration through the mevalonate pathway, knock down *SQLE* inhibited cell growth and migration [44]. Kim reported clinically collecting blood samples from POF patients younger than 40 years old, extracting genomic DNA, and analysing the DNA after purification [45]. The allele and genotype distribution revealed an interaction between an SNP in *FSHR* and two SNPs in *CYP19A1*, which are strongly associated with POF. In addition, *Adipoq* can activate AMPK by binding to *AdipoR1,* phosphorylating HMG-CoA reductase (HMGCR) in adipose tissue to inhibit the synthesis of diglycerides and triglycerides and inhibit cholesterol synthesis [46]. The underlying mechanisms for changes in steroid levels in POF mouse model have not been reported thus far.

In our study, the pathway enrichment results showed that the most direct and significant consequences of CTX were decrease in cholesterol biosynthesis pathway. Surprisingly, almost all the key genes needed in the cholesterol biosynthesis pathway are downregulated. In our PPI network, we showed that *SQLE* seemed to be a key target of CTX, and we speculated that CTX may play an anti-tumor role by inhibiting the activity of the *SQLE* gene and by down-regulating most of the key genes in the cholesterol biosynthesis pathway, such as *HMGCS1* and *HMGCR*, which both significantly regulate the rate of synthesis of acetyl-CoA to mevalonate during the biosynthesis of cholesterol. Simultaneously, the biological significance of hub genes (*Adipoq, APOA1, CYP19A1, GDF9* and *FSHR*) in the subnetwork should also attract more attention. *APOA1* and *Adipoq* regulate cholesterol production through the PPAR signaling pathway, *CYP19A1*, *GDF9* and *FSHR* regulate cholesterol production through the ovarian infertility genes pathway. Among these genes, the *CYP19A1* gene is the key link between cholesterol biosynthesis and ovarian infertility. It is a restriction enzyme for synthesis and has an elucidated association with *FSHR*. We also found that *CYP19A1* and *FSHR* were significantly increased in association with FSH expression.

5. Conclusion

We successfully construct a mouse model of POF by a single intraperitoneal injection of 70 mg/kg CTX, which showed typically pathological features. We also find that CTX may exert its anti-tumor effect by blocking the cholesterol biosynthesis pathway and cholesterol reduction is the initial cause of POF occurrence.

Declaration of competing interest

No competing financial interests exist.

Acknowledgments

This research was funded by National Key R&D Program of China, grant number 2017YFA0104400, and Program for Changjiang Scholars and Innovative Research Team in University, grant number IRT_16R32.

Appendix A. Supplementary data

Supplementary data to this article can be found online at https://doi.org/10.1016/j.lfs.2019.116999.

References

[1] A.M. Gonzalez-Angulo, F. Morales-Vasquez, G.N. Hortobagyi, Overview of resistance to systemic therapy in patients with breast cancer, Adv. Exp. Med. Biol. 608 (2007) 1–22 https://link.springer.com/chapter/10.1007%2F978-0-387-74039-3_1.
[2] T. Liu, S. Wang, Q. Li, Y. Huang, C. Chen, J. Zheng, Telocytes as potential targets in a cyclophosphamide-induced animal model of premature ovarian failure, Mol. Med. Rep. 9 (2016) 2415–2422 https://www.ncbi.nlm.nih.gov/pmc/articles/PMC4991733/.
[3] K.B. Kumar, R. Kuttan, Chemoprotective activity of an extract of Phyllanthus amarus against cyclophosphamide induced toxicity in mice, Phytomedicine 6 (2005) 494–500.
[4] H. Ren, P. Shen, X. Li, X. Pan, W. Zhang, N. Chen, Tacrolimus versus cyclophosphamide in steroid-dependent or steroid-resistant focal segmental glomerulosclerosis: a randomized controlled trial, Am. J. Nephrol. 37 (2013) 84–90 https://www.karger.com/Article/FullText/346256.
[5] M. Sun, S. Wang, Y. Li, L. Yu, F. Gu, C. Wang, Y. Yao, Adipose-derived stem cells improved mouse ovary function after chemotherapy-induced ovary failure, Stem Cell Res. Ther. 4 (4) (2013) 80.
[6] J. Waxman, Chemotherapy and the adult gonad: a review, J. R. Soc. Med. 76 (1983) 144–148 https://www.ncbi.nlm.nih.gov/pmc/articles/PMC1438671/.
[7] D. Meirow, H. Biederman, R.A. Anderson, W.H. Wallace, Toxicity of chemotherapy and radiation on female reproduction, Clin. Obstet. Gynecol. 53 (2010) 727–739 https://insights.ovid.com/pubmed?pmid=21048440.
[8] O. Oktem, K. Oktay, Quantitative assessment of the impact of chemotherapy on ovarian follicle reserve and stromal function, Cancer 110 (2007) 2222–2229.
[9] D. Goswami, G.S. Conway, Premature ovarian failure, Hum. Reprod. Update 11 (2005) 391–410 https://academic.oup.com/humupd/article/11/4/391/874983.
[10] P. Desmeules, P.J. Devine, Characterizing the ovotoxicity of cyclophosphamide metabolites on cultured mouse ovaries, Toxicol. Sci. 90 (2) (2006) 500–509 https://academic.oup.com/toxsci/article/90/2/500/1658405.
[11] S.G. Lopez, U. Luderer, Effects of cyclophosphamide and buthionine sulfoximine on ovarian glutathione and apoptosis, Free Radic. Biol. Med. 36 (11) (2004) 1366–1377.
[12] L. Zhou, Y. Xie, S. Li, Y. Liang, Q. Qiu, H. Lin, Q. Zhang, Rapamycin prevents cyclophosphamide-induced over-activation of primordial follicle pool through PI3K/Akt/mTOR signaling pathway in vivo, J. Ovarian Res. 8 (2017) 56 https://www.ncbi.nlm.nih.gov/pmc/articles/PMC5559863/.
[13] S. Senthilkumar, S.K. Yogeeta, R. Subashini, T. Devaki, Attenuation of cyclophosphamide induced toxicity by squalene in experimental rats, Chem. Biol. Interact. 4 (2006) 252–260 https://www.sciencedirect.com/science/article/pii/S0009279706000366?via%3Dihub.
[14] Z. Blumenfeld, N. Haim, Prevention of gonadal damage during cytotoxic therapy, Ann. Med. 29 (3) (1997) 199–206 https://www.tandfonline.com/doi/abs/10.3109/07853899708999337.
[15] M. Myers, K.L. Britt, N.G. Wreford, F.J. Ebling, J.B. Kerr, Methods for quantifying follicular numbers within the mouse ovary, Reproduction 5 (2004) 569–580 https://rep.bioscientifica.com/view/journals/rep/127/5/1270569.xml.
[16] M.E. Ritchie, B. Phipson, D. Wu, Y. Hu, C.W. Law, W. Shi, G.K. Smyth, Limma powers differential expression analyses for RNA-sequencing and microarray studies, Nucleic Acids Res. 4 (2015) e47 https://www.ncbi.nlm.nih.gov/pmc/articles/PMC4402510/.
[17] T.R. Derrick, B.T. Bates, J.S. Dufek, Evaluation of timeseries data sets using the Pearson product-moment correlation coefficient, Med. Sci. Sport. Exerc. 26 (1994) 919–928 https://insights.ovid.com/pubmed?pmid=7934769.
[18] P. Shannon, A. Markiel, O. Ozier, N.S. Baliga, J.T. Wang, D. Ramage, N. Amin, B. Schwikowski, T. Ideker, Cytoscape: a software environment for integrated models of biomolecular interaction networks, Genome Res. 13 (2003) 2498–2504 https://www.ncbi.nlm.nih.gov/pmc/articles/PMC403769/.
[19] W.Q. He, J.W. Gu, C.Y. Li, Y.Q. Kuang, B. Kong, L. Cheng, J.H. Zhang, J.M. Cheng, Y. Ma, The PPI network and clusters analysis in glioblastoma, Eur. Rev. Med. Pharmacol. Sci. 12 (2015) 4784–4790 https://www.europeanreview.org/article/10032.
[20] D. Liang, L. Li, C. Lynch, B. Mackowiak, W.D. Hedrich, Y. Ai, Y. Yin, S. Heyward, M. Xia, H. Wang, F. Xue, Human constitutive androstane receptor agonist DL5016: a novel sensitizer for cyclophosphamide-based chemotherapies, Eur. J. Med. Chem. 179 (2019) 84–99 https://www.sciencedirect.com/science/article/pii/S0223523419305598?via%3Dihub.
[21] I. El-Serafi, P. Afsharian, A. Moshfegh, M. Hassan, Y. Terelius, Cytochrome P450 oxidoreductase influences CYP2B6 activity in cyclophosphamide bioactivation, PLoS One 10 (11) (2015 Nov 6) e0141979https://www.ncbi.nlm.nih.gov/pmc/

articles/PMC4636385/.
[22] L. Detti, R.A. Uhlmann, M. Lu, M.P. Diamond, G.M. Saed, N.M. Fletcher, J. Zhang, L.J. Williams, Serum markers of ovarian reserve and ovarian histology in adult mice treated with cyclophosphamide in pre-pubertal age, J. Assist. Reprod. Genet. 11 (2013) 1421–1429 https://www.ncbi.nlm.nih.gov/pmc/articles/PMC3879939/.
[23] R. Jeelani, S.N. Khan, F. Shaeib, H.R. Kohan-Ghadr, S.R. Aldhaheri, T. Najafi, M. Thakur, R. Morris, H.M. Abu-Soud, Cyclophosphamide and acrolein induced oxidative stress leading to deterioration of metaphase II mouse oocyte quality, Free Radic. Biol. Med. 9 (2017) 11–18 https://www.sciencedirect.com/science/article/pii/S0891584917305798?via%3Dihub.
[24] J. Dynes, K. Osz, A. Hooper, J. Petrik, Low-dose metronomic delivery of cyclophosphamide is less detrimental to granulosa cell viability, ovarian function, and fertility than maximum tolerated dose delivery in the mouse, Biol. Reprod. 9 (2017) 449–465 https://academic.oup.com/biolreprod/article/97/3/449/4097578.
[25] W.R. Russell, A.L. Walpole, A.P. Labhsetwar, Cyclophosphamide: induction of superovulation in rats, Nature 1 (1973) 129–130 https://www.ncbi.nlm.nih.gov/pubmed/4695540.
[26] D.R. Plowchalk, D.R. Mattison, Reproductive toxicity of cyclophosphamide in the C57BL/6N mouse: 1. Effects on ovarian structure and function, Reprod. Toxicol. 6 (1992) 411–421 https://www.ncbi.nlm.nih.gov/pubmed/1463921.
[27] T. Liu, Y. Huang, L. Guo, W. Cheng, G. Zou, CD44 + /CD105 + human amniotic fluid mesenchymal stem cells survive and proliferate in the ovary long-term in a mouse model of chemotherapy-induced premature ovarian failure, Int. J. Med. Sci. 9 (2012) 592–602 https://www.ncbi.nlm.nih.gov/pmc/articles/PMC3461764/.
[28] T. Liu, S. Wang, L. Zhang, L. Guo, Z. Yu, C. Chen, J. Zheng, Growth hormone treatment of premature ovarian failure in a mouse model via stimulation of the Notch-1 signaling pathway, Exp. Ther. Med. 7 (2016) 215–221 https://www.ncbi.nlm.nih.gov/pmc/articles/PMC4906989/.
[29] T. Liu, Y. Huang, J. Zhang, W. Qin, H. Chi, J. Chen, Z. Yu, C. Chen, Transplantation of human menstrual blood stem cells to treat premature ovarian failure in mouse model, Stem Cells Dev. 7 (2014) 1548–1557 https://www.ncbi.nlm.nih.gov/pmc/articles/PMC4066227/.
[30] Y. Xiong, T. Liu, S. Wang, H. Chi, C. Chen, J. Zheng, Cyclophosphamide promotes the proliferation inhibition of mouse ovarian granulosa cells and premature ovarian failure by activating the lncRNA-Meg3-p53-p66Shc pathway, Gene 1 (2017) 1–8 (https://www.sciencedirect.com/science/article/pii/S037811191630806X?via%3Dihub.
[31] L. Casarini, P. Crépieux, Molecular mechanisms of action of FSH, Front. Endocrinol. 14 (10) (2019) 305 https://www.ncbi.nlm.nih.gov/pmc/articles/PMC6527893/.
[32] K.J. Juárez-Rendón, J.E. García-Ortiz, Evaluation of four genes associated with primary ovarian insufficiency in a cohort of Mexican women, J. Assist. Reprod. Genet. 35 (8) (2018) 1483–1488 https://www.ncbi.nlm.nih.gov/pmc/articles/PMC6086783/.
[33] W. Kaewlert, C. Sakonsinsiri, N. Namwat, K. Sawanyawisuth, P. Ungarreevittaya, N. Khuntikeo, N. Armartmuntree, R. Thanan, The importance of CYP19A1 in estrogen receptor-positive cholangiocarcinoma, Horm. Canc. 9 (6) (2018) 408–419 https://link.springer.com/article/10.1007%2Fs12672-018-0349-2.
[34] L. Miao, C. Jiao, R. Shao, Y. Qi, G. Fan, X. Li, Y. Wang, Y. Zhu, J. Zhang, X. Gao, Bakuchiol suppresses oestrogen/testosterone-induced Benign Prostatic Hyperplasia development through up-regulation of epithelial estrogen receptor β and down-regulation of stromal aromatase, Toxicol. Appl. Pharmacol. 381 (2019) 114637 https://www.sciencedirect.com/science/article/pii/S0041008X19302455?via%3Dihub.
[35] N.D. Shaw, S.N. Histed, S.S. Srouji, J. Yang, H. Lee, J.E. Hall, Estrogen negative feedback on gonadotropin secretion: evidence for a direct pituitary effect in women, J. Clin. Endocrinol. Metab. 95 (4) (2010) 1955–1961 https://www.ncbi.nlm.nih.gov/pmc/articles/PMC2853991/.
[36] K. Jankowska, Premature ovarian failure, Prz. Menopauzalny 16 (2017) 51–56 https://www.ncbi.nlm.nih.gov/pmc/articles/PMC5509972/.
[37] S. Wang, L. Yu, M. Sun, S. Mu, C. Wang, D. Wang, Y. Yao, The therapeutic potential of umbilical cord mesenchymal stem cells in mice premature ovarian failure, BioMed Res. Int. (2013) 690491 https://www.ncbi.nlm.nih.gov/pubmed/23998127.
[38] S.E. Charif, P.I.F. Inserra, A.R. Schmidt, N.P. Di Giorgio, S.A. Cortasa, C.R. Gonzalez, V. Lux-Lantos, J. Halperin, A.D. Vitullo, V.B. Dorfman, Local production of neurostradiol affects gonadotropin-releasing hormone (GnRH) secretion at mid-gestation in Lagostomus maximus (Rodentia, Caviomorpha), Phys. Rep. 10 (19) (2017) 5 https://www.ncbi.nlm.nih.gov/pmc/articles/PMC5641931/.
[39] S. Gill, J. Stevenson, I. Kristiana, A.J. Brown, Cholesterol-dependent degradation of squalene monooxygenase, a control point in cholesterol synthesis beyond HMG-CoA reductase, Cell Metabol. 3 (2011) 260–273 https://www.sciencedirect.com/science/article/pii/S1550413111000404?via%3Dihub.
[40] T.Z. Parris, A. Kovacs, S. Hajizadeh, S. Nemes, M. Semaan, M. Levin, P. Karlsson, K. Helou, Frequent MYC coamplification and DNA hypomethylation of multiple genes on 8q in 8p11-p12-amplified breast carcinomas, Oncogenesis 3 (2014) e95 https://www.ncbi.nlm.nih.gov/pmc/articles/PMC4038389/.
[41] J.J. Souchek, M.J. Baine, C. Lin, S. Rachagani, S. Gupta, S. Kaur, K. Lester, D. Zheng, S. Chen, L. Smith, A. Lazenby, S.L. Johansson, M. Jain, S.K. Batra, Unbiased analysis of pancreatic cancer radiation resistance reveals cholesterol biosynthesis as a novel target for radiosensitisation, Br. J. Canc. 111 (2014) 1139–1149 https://www.ncbi.nlm.nih.gov/pmc/articles/PMC4453840/.
[42] H.F. Yuen, C.M. McCrudden, Y.H. Huang, J.M. Tham, X. Zhang, Q. Zeng, S.D. Zhang, W. Hong, TAZ expression as a prognostic indicator in colorectal cancer, PLoS One 8 (2013) e54211https://www.ncbi.nlm.nih.gov/pmc/articles/PMC3553150/.
[43] J.H. Kim, C.N. Kim, D.W. Kang, Squalene epoxidase correlates E-cadherin expression and overall survival in colorectal cancer patients: the impact on prognosis and correlation to clinicopathologic features, J. Clin. Med. 8 (5) (2019) 8 pii: E632 https://www.ncbi.nlm.nih.gov/pmc/articles/PMC6572612/.
[44] Z. Sui, J. Zhou, Z. Cheng, P. Lu, Squalene epoxidase (SQLE) promotes the growth and migration of the hepatocellular carcinoma cells, Tumor Biol. 36 (2015) 6173–6179 https://www.ncbi.nlm.nih.gov/pubmed/25787749.
[45] S. Kim, J.A. Pyun, D.H. Cha, J.J. Ko, K. Kwack, Epistasis between FSHR and CYP19A1 polymorphisms is associated with premature ovarian failure, Fertil. Steril. 95 (2011) 2585–2588 https://www.ncbi.nlm.nih.gov/pubmed/21269619.
[46] A. Efeyan, W.C. Comb, D.M. Sabatini, Nutrient-sensing mechanisms and pathways, Nature 517 (2015) 302–310 https://www.ncbi.nlm.nih.gov/pubmed/25592535.